V. QUANTUM ELECTRONICS

A. Laser Applications

Academic and Research Staff

Prof. Shaoul Ezekiel
Dr. Robert E. Grove

Graduate Students

Salvatore R. Balsamo
Stephan C. Goldstein
Richard P. Hackel
Antonio C. Pires
George W. Sparks, Jr.
Frederick Y-F. Wu

1. MEASUREMENT OF THE SPECTRUM OF RESONANCE FLUORESCENCE FROM A TWO-LEVEL ATOM IN AN INTENSE MONOCHROMATIC FIELD

JSEP

Joint Services Electronics Program (Contract DAAB07-75-C-1346)

Shaoul Ezekiel, Robert E. Grove, Frederick Y-F. Wu

The spectrum of resonance fluorescence emitted by a carefully prepared two-level atomic system has been measured. The data were in good agreement with the theoretically predicted spectrum.[1,2]

The $3\,^2S_{1/2}$ $(F=2)$-$3\,^2P_{3/2}$ $(F'=3)$ transition in atomic sodium was prepared as a two-level system by optical pumping of the degenerate magnetic sublevels with resonant circularly polarized laser light. In this way we were able to excite the $m_F = 2$-$m_{F'} = 3$ transition selectively, thereby avoiding the complication caused by unequal matrix elements that connect other pairs of sublevels.

In our experimental arrangement a single-frequency cw dye laser is split into parallel "pump" and "signal" beams, which are separated by 1.2 cm and intersect an atomic beam of sodium at right angles. The pump beam prepares the F = 2 ground-state atoms in the $m_F = 2$ sublevel before they interact with the intense signal beam. A weak magnetic field (0.7 G) parallel to the laser beams is required to prevent redistribution of the sublevel populations by stray fields in the region between laser beams. The flouresecence induced by the signal beam is collimated and analyzed by a Fabry-Perot interferometer with a 2-MHz instrument width.

Figure V-1e shows the on-resonance spectrum for σ^+ polarization taken with an intensity of 640 mW/cm^2 and Fig. V-1d and V-1f are off-resonance spectra taken at the same intensity for detunings of -50 MHz and +50 MHz, respectively. Figure V-1a, 1b, 1c are corresponding theoretical plots using the measured Rabi frequency of 78 MHz taken from Fig. V-1e. The vertical lines in Fig. V-1a and V-1c represent the elastic scattering delta function, whose area is 0.46 times the total area of the spectrum. The elastic

JSEP

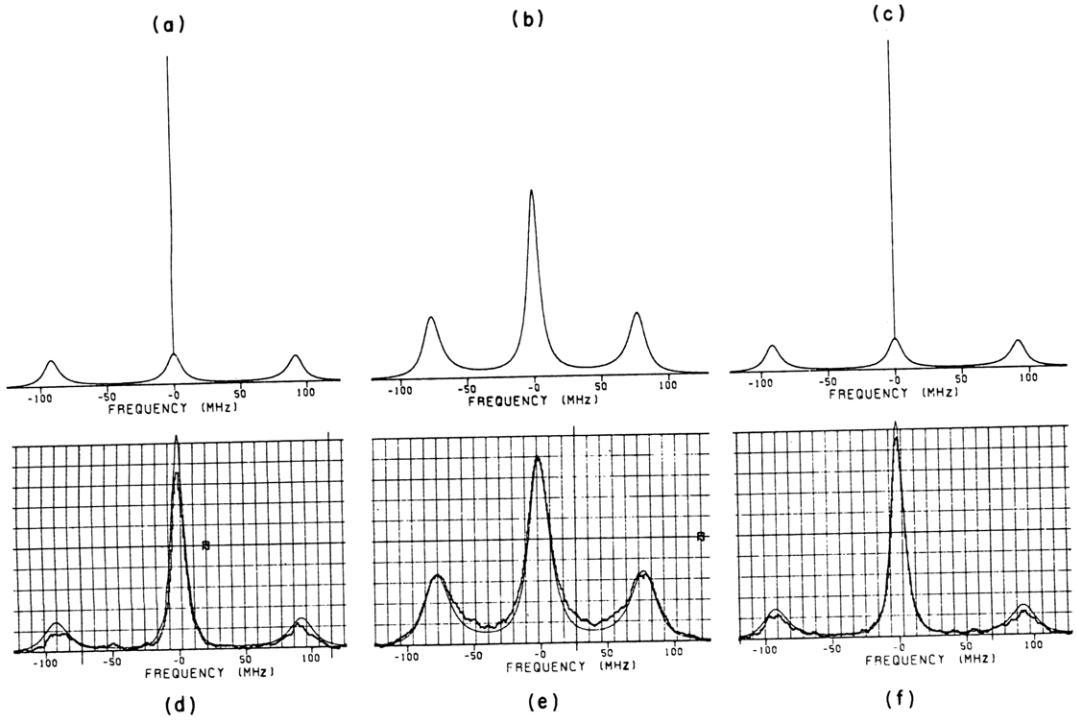

Fig. V-1. Theoretical and measured spectra for on- and off-resonance excitation.

scattering in the on-resonance spectrum is negligible at this field strength. To record the on-resonance spectrum, the pump and signal beams are locked to the F = 2-F' = 3 transition. For off-resonance spectra, an acousto-optic shifter is placed in the pump beam, and the laser is stabilized so that the shifted pump beam frequency is resonant with the F = 2-F' = 3 transition, and thus the signal beam is held at an accurately known detuning from resonance.

For a comparison of theory with experiment, we computed the convolution of the theoretical spectra of Fig. V-1a, 1b, 1c with the 9.5 MHz wide instrumental line shape of our arrangement. The instrumental line shape, which includes Doppler and Fabry-Perot broadening, was determined by observing the weak field (elastic scattering) spectrum, which ideally is a delta function. The convolved spectra are plotted as the smooth curves in Fig. V-1d, 1e, 1f; the vertical scale was chosen to make the central peak heights of the on-resonance experimental and convolved spectra equal.

References

1. B. R. Mollow, Phys. Rev. 188, 1969-1975 (1969).
2. Earlier attempts at measuring the spectrum have been reported by F. Schuda, C. R. Stroud, and M. Hercher, J. Phys. B 7, 198 (1974); H. Walther, in S. Haroche et al. (Eds.), Laser Spectroscopy (Springer Verlag, Berlin, Heidelberg, New York, 1975); F. Y. Wu, R. E. Grove, and S. Ezekiel, Phys. Rev. Letters 35, 1426 (1975).

V. QUANTUM ELECTRONICS

B. Gaseous Lasers

Academic and Research Staff

Prof. Hermann A. Haus
John J. McCarthy

Graduate Students

Peter L. Hagelstein
W. Michael Lipchak
David W. Wildman

1. IMPROVED FREQUENCY STABILITY OF THE TEA CO_2 LASER

JSEP

Joint Services Electronics Program (Contract DAAB07-75-C-1346)

W. Michael Lipchak

A previous investigation[1,2] of the temporal and spectral character of infrared laser radiation from the transversely excited, atmospheric (TEA) pressure CO_2 laser revealed severe frequency variations, during individual pulses, in the form of chirping of the order of 100 MHz/μs. Since typical pulses from the laser have peak powers in tens of kilowatts and 1-4 μs durations, the most significant chirp mechanism is hypothesized to be a change in the resonant electric susceptibility of the laser gain medium as its population inversion depletes rapidly during pulse formation.

This is a report of research[3] in support of this hypothesis that demonstrates improved frequency stability of the TEA CO_2 laser. The resonant electric susceptibility of a gain medium becomes increasingly insensitive to the degree of population inversion as the frequency of the field approaches the center frequency of the gain line. In fact, the resonant electric susceptibility is a constant, zero, for incident radiation that is precisely at the center frequency. If the hypothesis is accurate, then it is necessary to tune the frequency of the laser field, which is determined for the most part by the laser cavity resonance, to the center frequency of the gain spectrum of the medium, in order to effect a reduction in chirping.

Figure V-2 shows the experimental arrangement. The TEA laser is a gain tube, 1 m long, suspended in a 2 m resonant cavity. The tube contains a flowing gas mixture, $He:CO_2:N_2$ :: 2.1:1:.52, at 235 Torr total pressure. This mixture is excited, at a pulse rate of ~.5 Hz, by discharging a .025 μF capacitor bank across 166 diametrically opposed electrode pairs (1 in. gap), evenly spaced on the length of the gain tube. The "hot" side of each electrode pair is a 1 kΩ resistor. The capacitor charging voltage is 19 kV. The resonant cavity is defined by a flat aluminum diffraction grating and an 85% reflecting, solid germanium mirror with 4-m radius of curvature. The cavity length can be finely

JSEP

JSEP

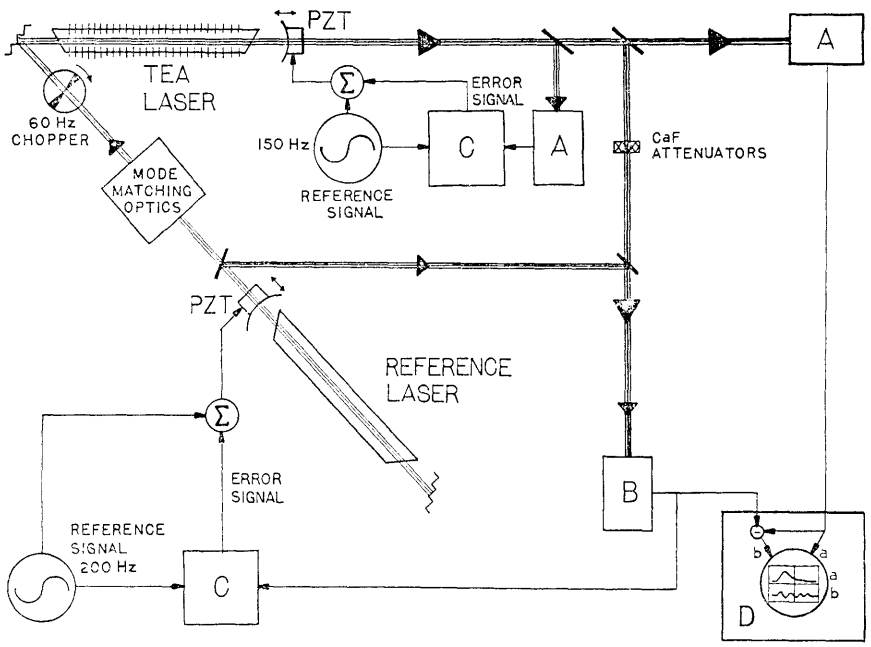

Fig. V-2. Diagram of experiment. A, IR detector; Ge:Au crystal in liquid nitrogen filled dewar. B, IR detector; Ge:Cu crystal in liquid helium filled dewar. C, synchronous detector and amplifier (Princeton Applied Research lock-in amplifier). D, Tektronix Type 556 dual-beam oscilloscope with Type 1A1 plug-in units.

tuned by adjusting the voltage applied to a piezoelectric transducer (PZT) upon which the curved mirror is mounted. The TEA laser is forced by the grating to operate in the P(18) vibrational-rotational transition of the 10.6 μm laser band.

The reference laser shown in Fig. V-2 is a typical flowing-gas, cw, CO_2 laser with ~2 W output power. Its cavity is also defined by a diffraction grating adjusted to force laser operation in the same gain transition, P(18), as the TEA laser. Its output mirror is also mounted on a PZT for fine tuning of the cavity length.

Since the reference laser contains a gain mixture under low pressure (12 Torr), it has a gain spectrum in the P(18) line that is only ~60 MHz wide (FWHM). Modulation of the cavity length at frequency ω_m, by application of a sinusoidal voltage component to the PZT, causes intensity modulations of frequency, ω_m to appear in the detected signal from that laser. An electronic feedback loop, consisting of a synchronous detector and amplifiers, attempts to minimize this detected modulation by adjusting the PZT bias voltage. The intensity modulation component at frequency ω_m, the fundamental, will be zero when the laser frequency is at the peak of the gain spectrum. In this manner the cw laser becomes a reference source that is very nearly at the center of the gain line of the CO_2 gain medium.

JSEP

Likewise, modulation of the TEA laser cavity length when the reference laser is

incident upon this cavity results in modulation of the transmitted intensity via the Fabry-Perot interferometry effect. This effect is maximized by matching the Gaussian beam parameters of the reference laser beam with those of the fundamental TEA laser cavity mode at the point of incidence, the diffraction grating. These intensity modulations are used again as a feedback signal to bring the fundamental TEA laser cavity mode almost into resonance with the energy transition of the gain medium. The precision of this tuning is limited by the gain and bandwidth of the electronic feedback loop and the amplitude of noise appearing in the detected signals. JSEP

The firing of the TEA laser is synchronized to periods during which the chopper shown in Fig. V-2 isolates the two laser resonators. Furthermore, the TEA laser signal is attenuated by CaF to result in an amplitude close to that of the reference laser. Under the assumption of stability in the cw laser during the period of a TEA laser pulse, the time-resolved frequency behavior of individual pulses is obtained by mixing the outputs of the two lasers and observing the beat frequency between them.

Typical oscillograms of the observed signals are shown in Fig. V-3. In Fig. V-3a, the upper trace is a typical (attenuated) TEA laser pulse and the lower trace is the same pulse mixed with the reference. A data set of beat signal phase vs time points was measured from each of 25 oscillograms showing beat signals. Each point is the time of occurrence of a relative minimum or maximum in the beat signal oscilloscope trace, estimated to within 1/120 μs. A linear regression on beat signal phase was performed for each data set. The derivative of each such regression is an estimate of the average beat frequency that is evident in the associated oscillogram. These 25 average beat

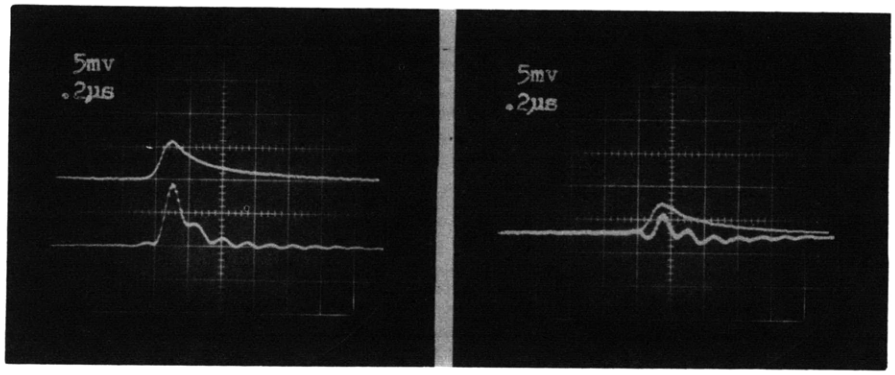

Fig. V-3. Sample oscilloscope photographs. (a) Upper trace: typical TEA laser pulse. Lower trace: same pulse mixed with the cw reference laser signal. (b) Similar pulse except that the pulse in the upper trace has been subtracted from the mixed signal and displayed in the lower trace.

JSEP

JSEP

frequencies are grouped in the neighborhood of 8 MHz. This is an indication of the typical separation of the two lasers in frequency and also suggests the order of the frequency offset of the TEA laser from resonance with the transition of the gain medium.

To obtain increased accuracy in visually identifying the minima and maxima of beat signals that are evident in the oscillograms, the pulse envelope was subtracted from the mixed signal by using the invert and add features of the oscilloscope. A typical oscillogram obtained in this manner is shown in Fig. V-3b. The upper trace is the pulse envelope and the lower is the beat signal after the envelope is subtracted from the mixed signal. Fourteen oscillograms, including Fig. V-3b, were taken and a data set of beat signal phase vs time points was measured from each. The results of the analysis of these 14 data sets, containing an average of 11 points for each, are summarized in Table V-1.

Table V-1. Summary of analysis of results.

Set	Goodness-of-Fit to Straight Line (%)	Lower Chirp Limit (MHz/μs)	Estimated Chirp Value (MHz/μs)	Upper Chirp Limit (MHz/μs)
1	99.24	-0.476	0.781	2.04
2	99.96	-3.77	0.888	5.54
3	99.04	2.2	2.345	2.49
4	99.96	-0.596	0.47	1.54
5	99.88	1.28	1.882	2.48
6	99.62	-6.2	-3.714	-1.22
7	99.34	-2.51	-1.85	-1.18
8	99.92	-2.78	-2.375	-1.97
9	99.92	0.391	1.542	2.69
10	99.92	-3.99	-1.413	1.17
11	99.98	-0.812	0.152	1.12
12	99.90	0.751	1.381	2.01
13	99.82	1.15	2.283	3.42
14	99.96	-0.432	1.03	2.49

A least-square-error straight line is fitted initially to each data set. The values of the Goodness-of-Fit[4] between straight lines and the data sets are tabulated. The second derivative of a beat signal phase vs time regression is an estimate of the average chirp occurring during the corresponding TEA laser pulse. Hence the very high degree of correlation to a straight-line fit indicates that the chirp in each data set should be extremely small.

JSEP

A second-order curve is then fitted to each data set and the second derivative of each curve, the estimated chirp value, is also listed in Table V-1. There is an uncertainty in each value that is due to the unavoidable inaccuracy in time measurements, and also to the length of each data set. This uncertainty is indicated by the minimum and maximum chirp limits listed in Table V-1 for each data set.

The estimated chirp values listed in Table V-1 demonstrate a significant improvement over previous observations.

References

1. W. A. Stiehl, "Measurement of the Spectrum of the TEA CO_2 Laser," S.M. Thesis, Department of Electrical Engineering, M. I. T., June 1972.
2. W. A. Stiehl and P. W. Hoff, "Measurement of the Spectrum of a Helical TEA CO_2 Laser," Appl. Phys. Letters 22, 680-682 (1973).
3. W. M. Lipchak, "TEA CO_2 Laser Frequency Stabilization," S.M. Thesis, Department of Electrical Engineering and Computer Science, M. I. T., May 1976.
4. J. C. Davis, Statistics and Data Analysis in Geology (John Wiley and Sons, Inc., New York, 1973), p. 197.

2. UNSTABLE RESONATORS IN MEDIA WITH PARABOLIC GAIN PROFILE

Joint Services Electronics Program (Contract DAAB07-75-C-1346)

Hermann A. Haus

An amplifying medium with a gain that decreases with the square of the distance from the axis (positive gain profile) supports "guided" modes of Gaussian profile that maintain the diameter as they propagate along the axis of the medium.[1,2] This effect has been used to achieve stable cavity modes in a mirror configuration that would otherwise be "unstable."[2] An analysis of an amplifying medium with a gain that increases with the square of the distance from the axis (negative gain profile) yields "steady-state" beam solutions that propagate without change of diameter.[1,2] These solutions, however, are unstable.[3] A negative gain profile is produced by gain saturation on the axis of the optical beam. Because of the unstable character of the "guided" solutions of a negative gain profile, focusing effects at the end mirrors of a plane-parallel resonator[4] cannot be attributed to cavity stabilization, but probably are attributable to the refractive effects of the gain medium coupled with discharge-tube wall reflection.

Two approaches lend themselves to achieving high cw output power with reproducible good mode quality in spite of the destabilizing effect of gain saturation: we may taper the transmissivity of the output mirrors,[5] or we may intentionally choose an unstable cavity configuration in which the optical beam profile is critically influenced by the

JSEP

mirror diameters. Even though gain saturation does not produce a parabolic gain profile, it is of interest to study unstable resonator configurations with parabolic gain profiles because useful insights can be obtained. In this report, we develop the formalism of unstable resonators in the presence of a parabolic gain profile and obtain closed-form solutions in the limit of large Fresnel number.

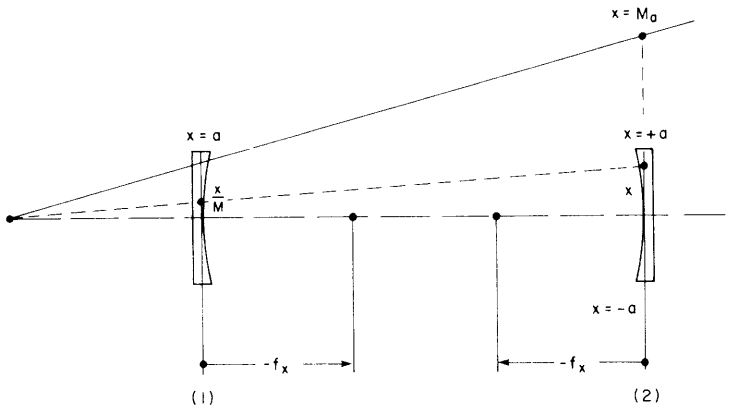

Fig. V-4. Unstable resonator (cross section in the y-z plane).

Consider the symmetric unstable resonator shown in Fig. V-4 with rectangular mirrors of focal distances f_x and f_y, respectively. The field pattern $\psi^{(2)}(x, y)$ at cross section (2) is represented[6,7] in terms of the pattern $\psi^{(1)}(x, y)$ at cross section (1) by

$$\psi^{(2)}(x, y) = \frac{jm}{\lambda \sin mL} \int_{-a}^{a} \int_{-b}^{b} dx_o dy_o \exp -j \frac{\pi}{\lambda} \left[\frac{m(x^2+y^2)}{\tan mL} - \frac{2m(xx_o+yy_o)}{\sin mL} + \frac{m\left(x_o^2+y_o^2\right)}{\tan mL} + \frac{x_o^2}{f_x} + \frac{y_o^2}{f_y} \right] \psi^{(1)}(x_o, y_o). \quad (1)$$

The kernel in (1) is the Green's function of the paraxial wave equation with a parabolic index profile[6]

$$\left(\frac{\partial^2}{\partial z^2}\right) \psi - \frac{4\pi \partial \psi}{j\lambda \partial z} - \left(\frac{2\pi}{\lambda}\right)^2 m^2 r^2 \psi = 0, \quad (2)$$

where m^2 is a measure of this parabolic index profile. The kernel in (2) is derived for

JSEP

a parabolic index profile,[6] and it is a simple matter to replace the dielectric constant,

and hence m^2, with a complex quantity. We look for eigenvalue solutions that are products of functions of x and y. Then the integrals separate and each factor may be worked on individually. The equation for the x-dependent part is

$$u^{(2)}(x) = \left(\frac{jm}{\lambda \sin mL}\right)^{1/2} \int_{-a}^{a} dx_o \exp - j\frac{\pi}{\lambda}\left[\frac{mx^2}{\tan mL} - \frac{2mxx_o}{\sin mL} + \frac{mx_o^2}{\tan mL} + \frac{x_o^2}{f_x}\right] u^{(1)}(x_o). \tag{3}$$

There is an analogous equation for the y-dependent part. In order to reduce the equation to standard form,[7] we write

$$u(x) = \exp\left[-A_x j\frac{\pi}{\lambda} x^2\right] v(x), \tag{4}$$

where A_x is so chosen that the eigenvalue equation for v assumes the form

$$v^{(2)}(x) = \gamma_x \left(\frac{jm}{\lambda \sin mL}\right)^{1/2} \int_{-a}^{a} dx_o \left\{\exp - j\frac{\pi}{\lambda}\left(m \cos mL + A_x + \frac{1}{f_x}\right)\left[x_o - \frac{x}{M_x}\right]^2\right\} v(x). \tag{5}$$

Here M_x is the "magnification" associated with the x variation, in general a complex quantity. The relations for A_x and M_x are

$$A_x = -\frac{1}{2f_x} \pm \sqrt{\left(\frac{1}{2f_x}\right)^2 - m^2 + \frac{m}{f_x \tan mL}} \tag{6}$$

and

$$M_x = \cos mL + \left(\frac{1}{2f_x} \pm \sqrt{\left(\frac{1}{2f_x}\right)^2 - m^2 + f_x \frac{m}{\tan mL}}\right)\frac{\sin mL}{m}. \tag{7}$$

The sign of the square root in (6) and (7) must be selected so that $|M_x| > 1$ because the (unstable) resonator mode, which is controlled by the mirror radii, must diverge continually as it bounces back and forth in the cavity. The choice of A_x is then dictated by the requirement $|M_x| > 1$.

When $\left|\frac{\pi}{\lambda}\frac{ma^2}{\tan mL}\right| \gg 1$ the exponential in (4) is a function that peaks sharply at $x/M = x_o$ and decreases rapidly to either side of this point, and it can be treated as a spatial impulse function. The integral can be carried out to obtain the result

$$v^{(2)}(x) = \gamma_x \frac{1}{(M_x)^{1/2}} v^{(1)}\left(\frac{x}{M_x}\right). \tag{8}$$

This is identical to Siegman's expression,[7] except that M_x is now complex. The eigenvalues are again

JSEP

$$v_n(x) = x^n, \qquad \gamma_x = \frac{1}{M_x^{n+1/2}}. \tag{9}$$

Consider the special case of plane-parallel mirrors, $f_x = \infty$. The resonator is unstable if the medium has a negative gain profile. Then $m^2 \rightarrow -j\mu^2$, where μ^2 is real and positive. From (6) we find

$$A_x = \pm\mu \frac{1}{\sqrt{2}} (1+j) \tag{10}$$

and

$$M_x = \exp \pm \frac{\mu}{\sqrt{2}} (1+j). \tag{11}$$

Because $M_x > 1$ we must choose the upper sign, and the lowest eigenmode has the form

$$v_o(x) = \exp +\mu \frac{\pi}{\lambda} x^2 \exp -j\mu \frac{\pi}{\lambda} x^2. \tag{12}$$

The mode amplitude increases toward the rim of the mirrors. This is to be expected for a medium that has the largest gain on the outside.

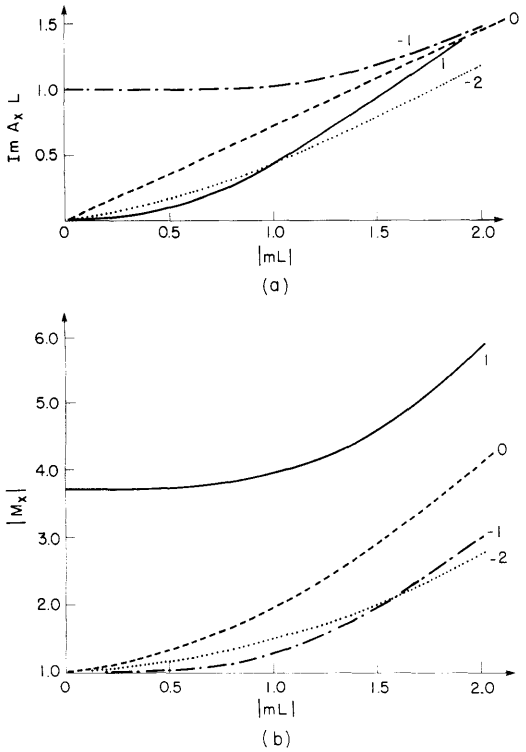

Fig. V-5.
(a) Magnification in the x-z plane, M_x, and (b) the exponential taper, $L\,\mathrm{Im}\,A_x$, as functions of $|mL|$, with $(L/2f_x)$ as parameter.

JSEP

Figure V-5 shows the gain M_x and the taper parameter Im A_x vs the parameter $|mL|$ for a gain medium of negative profile with $(L/2f_x)$ as a parameter. JSEP

For $(L/2f_x) = -1$, we find Im $A_x > 0$, even for $|mL| = 0$. This means that the mode has a radial profile, increasing away from the axis, contrary to what would be expected for the lowest order mode of an unstable resonator in vacuo. The explanation is as follows: When $(L/2f_x) = -1$, the resonator configuration is stable in vacuo. With $|M_x| > 1$ the mode pattern singles out the solution that grows exponentially away from the axis and is disregarded in the stable resonator case. This solution becomes legitimate when a gain profile is present, but has very high diffraction losses even for weak gain profiles. In the design of an unstable resonator with small diffraction loss one should keep away from the region of stability of the resonator in vacuo, $-2 \leq L/2f_x \leq 0$.

References

1. H. Kogelnik, "On the Propagation of Gaussian Beams of Light through Lenslike Media Including Those with a Loss or Gain Variation," Appl. Opt. 4, 1562 (1965).
2. L. Casperson and A. Yariv, "The Gaussian Mode in Optical Resonators with a Radial Gain Profile," Appl. Phys. Letters 12, 355 (1968).
3. U. Ganiel and Y. Silberberg, "Stability of Optical Resonators with an Active Medium," Appl. Opt. 14, 306-309 (1975).
4. W. J. Witteman and G. J. Ernst, "Gain Induced Stability of Active Plane-Parallel Resonators," Appl. Phys. (Germany) 6, 297-304 (1975).
5. U. Ganiel, A. Hardy, and Y. Silberberg, "Stability of Optical Laser Resonators with Mirrors of Gaussian Reflectivity Profiles, Which Contain an Active Medium," Opt. Commun. 14, 290-293 (1975).
6. S. A. Collins, Jr., "Lens System Diffraction Integral, Written in Terms of Matrix Optics," J. Opt. Soc. Am. 60, 1168-1177 (1970).
7. A. E. Siegman and R. Arrathoon, "Modes in Unstable Optical Resonators and Lens Waveguides," IEEE J. Quantum Electron., Vol. QE-3, No. 4, pp. 156-163, April 1967.

JSEP

V. QUANTUM ELECTRONICS

C. Nonlinear Phenomena

Academic and Research Staff

Prof. Hermann A. Haus
Dr. Fielding Brown

Graduate Students

Peter L. Hagelstein
Ping-Tong Ho

JSEP

1. STABILITY OF SOLUTIONS OF PASSIVE MODE LOCKING

Joint Services Electronics Program (Contract DAAB07-75-C-1346)

Hermann A. Haus, Peter L. Hagelstein

The recently developed theory of passive mode locking has led to closed-form solutions for passive mode locking of a laser.[1,2] The passive mode-locking solutions for a fast saturable absorber were tested for stability by investigating the initial growth (or decay) of the energy in a perturbation of varying width and height.[1] This test established a value of normalized small-signal gain g_o for each value of the absorber parameter, K, for which "stable" mode-locking solutions are to be expected. K is defined by

$$K = \frac{1}{4}\left(\frac{P_L}{P_A}\right)\omega_L T_p,$$

where P_L and P_A are the saturation powers of laser and absorber, respectively, ω_L is the linewidth of the laser, and T_p is the period of the pulse train. The boundary g_o vs K was used in establishing criteria for the system parameters required to achieve cw passive mode locking.[3]

Although, as we have pointed out,[1] the test of stability was not sufficient to establish stability against any perturbation, it was deemed to be satisfactory for the purpose, in particular, because physical reasoning suggested that the most dangerous perturbations were pulselike, with a single maximum coincident with the mode-locked pulse.

In spite of these arguments, it seemed desirable to conduct a test that would be sufficient to establish stability. Such a test, which requires the study of the initial time evolution of a perturbation of arbitrary shape, was performed by Hagelstein.[4] As expected, it was found that the stability boundary used by Haus[3] was very close to the correct one. Figure V-6 compares the locus of apices of the $1/\omega_L\tau_p$ vs K curves (Haus,[1] Fig. 2), which was used as the approximate stability boundary, with the exact stability boundary. The two are very close to each other. The surprising result is that

JSEP

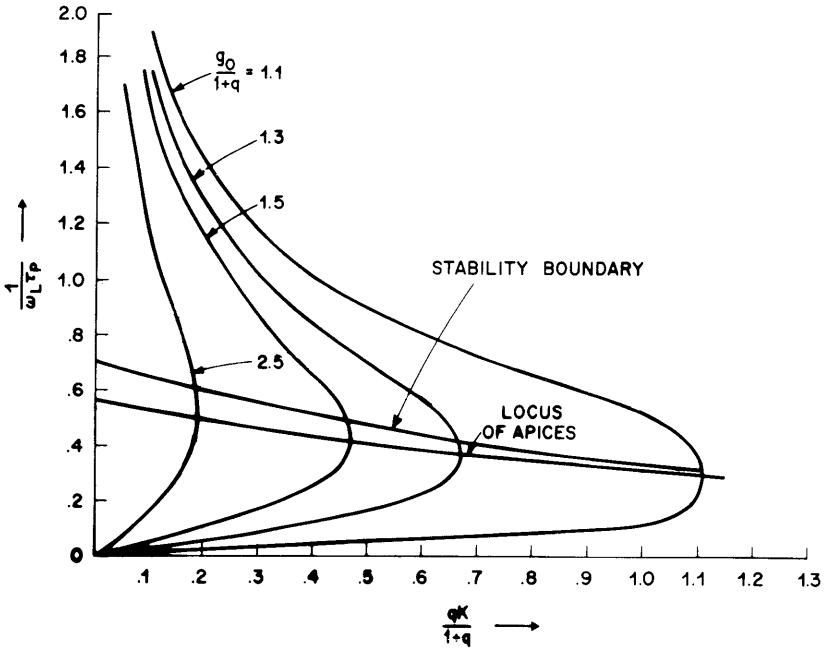

Fig. V-6. Stability boundary of mode-locked solution for a fast absorber. Solutions below the boundary are stable.

the actual stability boundary lies slightly above the locus of the apices, and hence in a very narrow regime two mode-locked solutions of slightly different width are found to be stable; the system is bistable. Whether this finding is of any practical significance is not yet clear because the difference between the two allowed solutions is very slight.

References

1. H. A. Haus, "Theory of Mode Locking with a Fast Saturable Absorber," J. Appl. Phys. 46, 3049-3058 (1975).

2. H. A. Haus, "Theory of Mode Locking with a Slow Saturable Absorber," IEEE J. Quantum Electron., Vol. QE-11, No. 9, pp. 736-746, September 1975.

3. H. A. Haus, "Parameter Ranges for cw Passive Mode Locking," IEEE J. Quantum Electron., Vol. QE-12, No. 3, pp. 169-176, March 1976.

4. P. L. Hagelstein, "Stability Analysis of a Passively Mode-Locked Laser System," S.M. Thesis, Department of Electrical Engineering and Computer Science, M.I.T., May 1976.